

Secondary Emission Enhanced Photoinjector

I. Ben-Zvi

April 2004

Collider Accelerator Department
Brookhaven National Laboratory

U.S. Department of Energy

USDOE Office of Science (SC)

Notice: This technical note has been authored by employees of Brookhaven Science Associates, LLC under Contract No. DE-AC02-98CH10886 with the U.S. Department of Energy. The publisher by accepting the technical note for publication acknowledges that the United States Government retains a non-exclusive, paid-up, irrevocable, world-wide license to publish or reproduce the published form of this technical note, or allow others to do so, for United States Government purposes.

DISCLAIMER

This report was prepared as an account of work sponsored by an agency of the United States Government. Neither the United States Government nor any agency thereof, nor any of their employees, nor any of their contractors, subcontractors, or their employees, makes any warranty, express or implied, or assumes any legal liability or responsibility for the accuracy, completeness, or any third party's use or the results of such use of any information, apparatus, product, or process disclosed, or represents that its use would not infringe privately owned rights. Reference herein to any specific commercial product, process, or service by trade name, trademark, manufacturer, or otherwise, does not necessarily constitute or imply its endorsement, recommendation, or favoring by the United States Government or any agency thereof or its contractors or subcontractors. The views and opinions of authors expressed herein do not necessarily state or reflect those of the United States Government or any agency thereof.

Secondary Emission Enhanced Photoinjector

Ilan Ben-Zvi^{1,2}, Xiangyun Chang¹, Peter D. Johnson²,
Jörg Kewisch¹, Triveni S. Rao³,
Collider-Accelerator Department¹, Physics Department²,
Instrumentation Division³
Brookhaven National Laboratory
Upton NY 11973 USA



**Collider-Accelerator Department
Brookhaven National Laboratory
Upton, NY 11973**

Secondary Emission Enhanced Photoinjector

Ilan Ben-Zvi^{1,2}, Xiangyun Chang¹, Peter D. Johnson², Jörg Kewisch¹, Triveni S. Rao³
Collider-Accelerator Department¹, Physics Department², Instrumentation Division³
Brookhaven National Laboratory
Upton NY 11973 USA

Abstract:

We report a new approach to the generation of high-current, high-brightness electron beams. Primary electrons are produced by a photocathode (or other means) and are accelerated to a few thousand electron-volts, then strike a specially prepared diamond window. The large Secondary Electron Yield (SEY) provides a multiplication of the number of electrons by about two orders of magnitude. The secondary electrons drift through the diamond under an electric field and emerge into the accelerating proper of the “gun” through a Negative Electron Affinity surface of the diamond.

The advantages of the new approach include the following: 1. Reduction of the number of primary electrons by the large SEY, i.e. a very low laser power in a photocathode producing the primaries. 2. Low thermal emittance due to the NEA surface and the rapid thermalization of the electrons. 3. Protection of the cathode from possible contamination from the gun, allowing the use of large quantum efficiency but sensitive cathodes. 4. Protection of the gun from possible contamination by the cathode, allowing the use of superconducting gun cavities. 5. Production of high average currents, up to ampere class. 6. Encapsulated design, making the “load-lock” systems unnecessary.

Section 1. Introduction

The creation of high average-current, high brightness electron beams is a key enabling technology for a large number of accelerator-based systems, such as ultra-high-power Free-Electron Lasers (FELs), Energy-Recovery Linac (ERL) light sources, electron cooling of hadron accelerators, and many more.

In order to produce the high brightness (or low emittance at high bunch charge), laser photocathode RF guns have proven performance that make them the ideal choice for devices like X-ray FELs. The high electric field that may be achieved in the RF gun is the key factor in getting a large charge with a small emittance.

The photocathode and its associated laser are, arguably the most difficult aspect of the laser-photocathode electron gun. Robust, metallic cathodes are popular in RF guns that operate at a very low average current. They are usually driven in the near UV (typically 0.25 microns wavelength, obtained by frequency quadrupling a 1 micron laser). The frequency quadrupling is itself a wasteful process. Semi-conducting photocathode can provide very high Quantum Efficiency (QE) at a longer wavelength, between 1 to 0.5 microns (IR to green light), making such cathode the natural candidates for high average current guns. The problem with these cathodes is twofold: They are very sensitive to any

contamination, thus must be prepared and maintained under ultra-high vacuum conditions and still may suffer a short lifetime if the vacuum in the gun is less than pristine. The other problem may be encountered in superconducting guns, where the chemicals of the cathode (most common is cesium) may degrade the superconducting gun surface. Finally, even with the extremely good QE of 10% available in green light with such cathodes, the CW laser is formidable, requiring a few 10's of watts CW with some exacting demands on pulse length, stability and more.

In order to produce a high average current, one has to operate the gun in a continuous mode (CW). That is easy with a DC guns, but the price to pay is a much lower electric field. The best duty factor demonstrated so far in normal conducting RF guns was 25%. Guns with 100% duty factor are in the works, but again the field strength is sacrificed due to the huge power that flows into the gun cooling system. The best candidate to a high-brightness, CW gun is the superconducting RF gun. However, the problem there is as stated above, the contamination of the gun by the cathode material.

We report a new approach to the generation of high-current, high-brightness electron beams. Primary electrons are produced by a laser-photocathode (or other means, as will be discussed later), are accelerated to a few thousand electron-volts, and then strike a specially prepared diamond window. The large Secondary Electron Yield (SEY) provides a multiplication of the number of electrons by about two orders of magnitude. The secondary electrons drift through the diamond under an electric field and emerge into the accelerating proper of the "gun" through a Negative Electron Affinity surface of the diamond. The accelerating field can be provided by the gun electrical field that penetrates the diamond window.

The advantages of the new approach include the following: 1. Reduction of the number of primary electrons by the large SEY, i.e. a very low laser power in a photocathode producing the primaries. 2. Low thermal emittance due to the NEA surface and the rapid thermalization of the electrons. 3. Protection of the cathode from possible contamination from the gun, allowing the use of large quantum efficiency but sensitive cathodes. 4. Protection of the gun from possible contamination by the cathode, allowing the use of superconducting gun cavities. 5. Production of high average currents, up to ampere class. 6. Encapsulated design, making the "load-lock" systems unnecessary.

Naturally, this cathode will be most suitable for a superconducting RF gun for CW operation, but it has significant advantages also for normal conducting, pulsed RF guns and DC guns. Therefore, in the following, we will describe the application of this new paradigm as applied to a superconducting RF gun and with the primary electron source being a cesium-potassium-antimonide cathode driven by a 0.5 micron laser. Extension to other guns and other cathodes is trivial.

The principle of the photo-multiplying cathode is as follows: The electrons in this gun can be generated by laser light illuminating a high-quantum efficiency photocathode, such as CsK₂Sb (cesium-potassium-antimonide). The cathode will be situated behind a thin (10 to 20 micron), specially prepared diamond window. The RF field of the cavity penetrates into a small gap (under 1 mm) between the photocathode and the diamond

window. The electrons are accelerated by this field to a few keV and strike the diamond. The electrons are stopped rapidly, generating a cascade of secondary electrons (depending on the primary energy, even 100 secondary electrons per primary have been measured). The secondary electrons drift through the diamond under the electrical field. The surface of the diamond on the superconducting cavity side is specially prepared by hydrogen bonding to be a Negative Electron Affinity (NEA) surface. Since the electrons are thermalized in passage through the diamond to sub eV temperature, the NEA surface allows them to exit the diamond with a very low thermal emittance.

The amount of primary electrons needed is about two orders of magnitude lower than the number of secondaries produced, thus the quantum efficiency of about 10% from CsK₂Sb will be translated to about 1000% quantum efficiency! This makes the laser, a traditionally difficult component of any photoinjector into a rather trivial device.

Most of the work on SEE from diamond has been in the reflection mode where the primary and secondary electrons are on the same side of the sample. For our application, the preferred option is the transmission mode, where the primary and secondary electrons are on opposite sides of the sample. In this mode, the production of the SEE takes place on one side (the side where the primary electrons impinge) and the emission takes place on the other side, thereby separating the two processes. That allows us to tailor the properties of the diamond on its two surfaces and in its bulk to optimize the various processes, such as the electrical conductivity of the material at the primary input surface for reducing the heat load due to the replenishment current, the thermal conductivity of the diamond bulk for waste heat removal and the secondary emission surface for best NEA conditions.

The low emittance possible with the thermalization of the electrons and the NEA surface combines with the high electric fields of the superconducting cavity (say 30 MV/m on the cathode) to produce a low space-charge emittance. In addition, the high thermal conductivity make diamond an ideal candidate for high current application. Thus a superconducting gun with a secondary emission enhanced photocathode will allow an extremely small emittance at very high current.

The photo-multiplying cathode with superconducting gun is thus the ideal electron generator for various projects such as the electron cooling of RHIC, a ERL light-source or megawatt class Free-Electron Lasers. Many other applications are possible, such as a compact, high-flux Compton-scattering device to produce short-pulse hard X-rays for medical diagnostics and industrial applications and extremely powerful terahertz radiation.

In the following sections, we address various design considerations for secondary emission enhanced photoinjector.

Section 2. The structure of a secondary emission enhanced photocathode.

There are many possible configurations for a secondary emission enhanced cathode. The basic principle is that primary electrons strike the backside of a diamond window at an energy of a few keV, a large number of secondary electrons are produced in the diamond, the secondary electrons are transported across the diamond by a superimposed electric field and the electrons emerge to the gun accelerating gap. Indeed, one can even enhance any electron source for primary electrons, including a pulsed thermionic electron source or even an X-ray source. The process of conversion of the primary electrons into secondary electrons wipes out the history of the primary electrons, leaving only a few characteristics: The current and bunch length of the primaries and the area of the diamond over which they are spread. Thus, for example, the emittance of the primary electrons is unimportant. Indeed, one can even cascade a few diamond secondary emission enhancing plates and use the output of one as the input to the next, increasing dramatically the current gain of the combined device. Such a cascaded secondary emission enhanced cathode can use a low power laser with a rugged but low quantum efficiency metallic cathode as the initial source of the primary electrons. However, for the sake of the discussion, we will assume that the source of the primary electrons is a photocathode illuminated by a laser pulse and that only a single stage of diamond secondary emission enhancer is used.

Likewise, the diamond secondary emission enhanced photocathode can be placed in either a DC electron gun or RF electron gun. The RF electron gun can be either a pulsed or CW device, normal-conducting or superconducting. Again, for the sake of the discussion we will assume a CW superconducting RF gun at 703.75 MHz. These parameters happen to be the parameters for the electron gun for the RHIC electron cooler.

Figure 1 shows a schematic layout of such a device.

The primary electrons originate in a photocathode, illuminated by a laser beam. Part of the cavity of the RF gun is shown. The cathode is mounted on a cathode stalk, which is thermally insulated from the gun cavity. For our example of a superconducting gun cavity the stalk may be cooled to liquid nitrogen temperature. A choke joint (not shown) provides electric continuity to the gun cavity and prevents leakage of RF field through the cathode stalk.

The electric field of the gun cavity penetrates the diamond and terminates on the photocathode. This field is quite high, of the order of 10 to 20 MV/m at the launch phase of the electrons from the photocathode (corresponding to about 30 MV/m peaks field). Thus, a gap of 0.5 mm between the photocathode and the diamond will provide over 5 to 10 keV of primary electrons at the time they strike the diamond.

An enlarged section of the diamond is shown as an inset. The diamond face accepting the primary electrons is coated with a very thin (about 10 nm or less) of gold. The purpose of the gold is to serve as an electric conductor to bring the current for replenishing the

diamond with the current that it emits. The gold is thin enough to be transparent to both the laser radiation and the cavity electric field. The secondary electrons are generated in RF Cavity

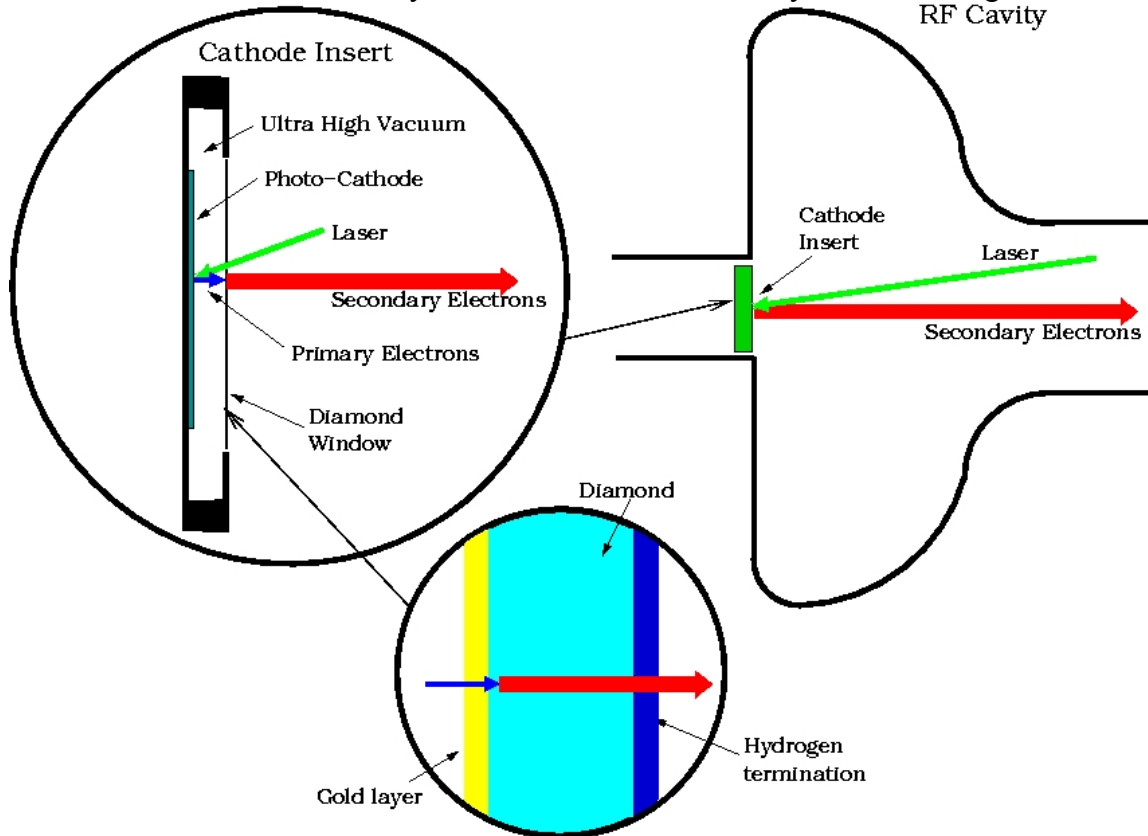


Figure 1. Schematic diagram of a secondary emission enhanced photoinjector. Please note that the figure is not to scale. The figure on top right shows the cathode insert in the gun cavity. The figure on top-left is a magnified view of the cathode insert. The gap between the diamond window and the photocathode is typically some fraction of a millimeter. The bottom figure is a blow-up of the diamond, showing (very schematically) a gold coating on the photocathode side of the diamond and hydrogen termination of the diamond's dangling bonds on the gun side of the diamond. The gold is very thin, about 10 nm or less, while the diamond may be as much as 10 microns thick, while the hydrogen is a monolayer.

the diamond window. Finally, the diamond face on the gun cavity side has the diamond dangling bonds terminated by hydrogen to provide a Negative Electron Affinity (NEA) surface. This serves to ease the secondary electrons exit into the gun cavity.

Section 3. Secondary electron yield and general properties

The physical and electronic properties of diamond make it a very attractive candidate for a high current, and high current density secondary electron emitter to be used in an RF injector.

- It has the highest high electric field electron and hole velocity [1] of $>10^7$ cm/s at 2 MV/m field, a gradient that would be present in an RF injector. Such a high velocity decreases the transit time of the secondary electrons through the medium.
- Ability of diamond to be doped to desired boron concentration and hence desired electrical resistivity, low trap density and high carrier mobility
- Hydrogenated, boron doped as well as undoped diamond has shown to have negative electron affinity [2,3] increasing the secondary electron yield. Indeed, Boron doped, hydrogenated polycrystalline diamond has been shown [4] to be an effective secondary emitter with an enhancement factor of > 80 .
- The energy distribution of the secondary electrons under low electric field is shown to be < 1 eV, centered ~ 4.5 eV above the Fermi energy. This energy distribution is larger than the thermal distribution of the electrons, leading one to conclude that the escape time is smaller [5] than the electron-phonon relaxation time of 10^{-12} - 10^{-13} s [6]. The secondary electrons energy distribution traversing the diamond will be the result of equilibrium. On one hand, the electric field pumps energy into the electrons and the elastic collisions randomize this energy. On the other hand the inelastic collisions remove thermal energy from the electrons and they tend towards the lattice temperature. This process is calculated below, and results a low electron temperature of about 0.1 eV. and a temporal width of ~ 1 ps, or with a slightly larger energy distribution, but narrower temporal width. In either case, the brightness of these electrons will be very high.
- Transport of low energy electrons through diamond has been shown to be very efficient [7]
- Thermal conductivity of diamond is in the range of 20 W/cmK at room temperature and even higher at LN2 temperature [8]. Dissipation of heat generated by the high-energy electrons as well as the high current becomes manageable with such high conductivity.

The thermal drift of electrons in gold is well known and is actually a very monotonic and slow function of the applied field. The thermal drift velocity at room temperature is known to be about 10^5 m/s for both pure and boron doped diamond. At fields of the order of a few MV/m, the drift velocity at room temperature is approximately 2×10^5 m/s. Data at room temperature were fitted to a straight line result

$$(2.1) \quad V_d = 10^5 (0.2E + 0.55)$$

where V_d is the drift velocity in m/s, E is the instantaneous electric field in the diamond in MV/m. This is just an approximation over a limited range around 1 to 2 MV/m, which is sufficient for our present purpose.

In the following, we will apply the diamond properties to calculate various parameters of the secondary electron beam.

Section 4. Secondary electron temperature

The inelastic mean free path IMFP of the electrons in the diamond and the acceleration by the electric field determine the equilibrium temperature attained by the drifting electrons. Since the IMFP is energy dependant, we must solve for the temperature and the inelastic mean free part simultaneously.

The equation for the equilibrium electron random energy E_e as a function of the inelastic mean free path λ_i and the lattice temperature T_l and the electric field in the diamond can be written as follows:

$$(4.1) \quad \frac{E_e - kT_l}{\tau_w} = -eEV_d$$

k is the Boltzmann constant, e is the electron's charge and E is the electric field in the diamond. V_d is the drift velocity and τ_w is the relaxation time of the electron's temperature to the lattice.

Neglecting the lattice temperature, and expressing the relaxation time as a function of the electron's thermal energy and the IMFP, we get

$$(4.2) \quad \frac{1}{2}mV_e^3 = -eEV_d\lambda_i$$

For the IMFP we will use the semi-empirical formula of M.P. Seah and W.A. Dench [9]

$$(4.3) \quad \lambda_i = \left[538E_r^{-2} + 0.41(a_m E_r)^{\frac{1}{2}} \right] a_m$$

where a_m is the thickness of a monolayer in nanometers, for diamond $a_m = 0.1783$ nm. E_r is the electron's energy above the Fermi level. At the low energies near equilibrium, the first term dominates. Expressing the energy above the Fermi level as

$$(4.4) \quad E_r = E_e + \Delta$$

where $\Delta = E_C - E_F$ is the energy of the conduction band above the Fermi energy, we can solve numerically equations (4.2) and (4.3). We will use the following values, a band gap of 5.5 eV and the Fermi energy is 2.725 eV below the conduction band. Thus $\Delta = 2.725$ eV. The solution of the equations for a field E of 2 MV/m results $E_e = 0.1$ eV, a comfortably low temperature. The corresponding IMFP is $\lambda_i = 12.5$ nm. The maximum energy that the electron can gain during one IMFP is $eE\lambda_i$, which is 0.025 eV.

Section 5. Transit time and temporal spread

The transit time of the electrons must be considered in an RF gun application, since this transit time appears as a delay between the arrival time of the primary electrons and the emergence of the secondary electrons into the gun. During this time the phase of the RF field is advancing and the various calculations must take this time dependence into account.

For a drift velocity of 1.5×10^5 m/s (see section 3 above), the time of flight thorough a 10 micron thick diamond is 66 ps, or about 17 degrees of phase at 703.75 MHz, a reasonable number. In fact, the mobility of electrons increases with lowered temperature, and that may reduce the flight time by a factor of 2 if the diamond temperature is reduced from 300°K to about 100°K (the mobility at low field increases more dramatically with lowered temperature, but at a few megavolts per meter the increase is smaller).

Another important consideration is the spread in the time of arrival of the secondary electrons at the far side of the diamond window. Most applications of electron guns place an upper limit on the final pulse width. There are two mechanisms that have to be considered.

The temporal spread can come from two sources. One is the random walk due to the thermal energy; the other is the space-charge induced bunch spread.

In the random walk part of the problem, we have to consider the mean free path of the electrons.

At very low energy most of the momentum modification of electrons takes place through elastic collisions. However, even if we totally neglect the elastic mean free path and assume that the electron executes a random walk with a velocity corresponding to the equilibrium thermal energy calculated in section 4, we get a quite short random walk. The velocity corresponding to the kinetic thermal energy of 0.03 eV is

$$(5.1) \quad v_t = 3 \times 10^8 \sqrt{\frac{2 \times 0.03}{0.511 \times 10^6}} = 10^5 \text{ m/s}$$

which is the published thermal drift velocity of electrons in diamond (with no electric field). For a diamond thickness of 10^{-5} m, the number of IMFP steps is $N = 5.6 \times 10^4$, and the rms random walk is given by $0.5 \cdot N^{0.5} \times 0.178 \times 10^{-9} / 10^5 = 2 \times 10^{-13}$ s, or about 0.2 ps. Thus we conclude that the thermal random walk of the electrons is negligible.

The space-charge induces the main temporal spread that we have to consider. The part that is different from what takes place in any high-bunch charge electron gun is that the electrons spend a period of time in the diamond, moving at a relatively low velocity. At the same time, the space charge fields are reduced by the dielectric constant of diamond, which is $\epsilon_r = 5.7$. The geometry of the diamond window facilitates the calculation, since the electrons are spread over a very thin, wide disk. A precise calculation should take into account the time dependence of the RF accelerating field, but for a rough estimate we can

approximate the field as constant (let us take $E=2$ MV/m in the diamond, which would correspond to $\epsilon_r E=5.7 \times 2$ MV/m external field). For the $R=5$ mm cathode radius, at a charge of $Q=1$ nC per bunch, the space charge electric field acting on either end of the bunch on account of the bunch-charge is

$$(5.2) \quad E_{sc} = \frac{Q}{\pi R^2 \epsilon_0 \epsilon_r}$$

or about 0.25 MV/m. Thus the head of the bunch will move under a field of 2.25 MV/m and the tail will move under a field of 1.75 MV/m. Now we can use equation (2.1) to calculate the resulting drift velocities of the head and tail, and the resulting time of flight. We find that, for room temperature, the head of the bunch will leave the diamond 10 ps ahead of the tail, in addition to the original bunch spread. At 703.75 MHz, this amounts to about 2.5 degrees. At 100°K, the effect is reduced to a totally negligible sub-degree spread.

Section 6. Thermal load on the diamond

Heat is generated by a number of sources:

- The energy deposited by the primary electrons.
- The current flowing through the gold electrode to replenish the escaped charge. It is easy to verify that even for a very thin gold layer of 10 nm thickness this is a negligible source of heat and will not be calculated here.
- Heat developed by the transit of the secondaries through the diamond.

We will evaluate these heat sources and estimate the temperature rise of the diamond, assuming it is cooled on the periphery to near liquid nitrogen temperature.

The primary electrons' heat load, P_p : Given that the secondary emission yield is approximately proportional to the primary energy, the heat generated by the primary electrons is nearly independent of their energy and depends only on the secondary electron current. Using the data for hydrogen terminated diamond [7], the secondary emission coefficient δ is 60 at $E_p=3$ keV primary energy. Let the primary current be I_p and the secondary current I_s , then

$$(6.1) \quad I_p = \frac{I_s}{\delta} = \frac{50I_s}{E_p}$$

Therefore

$$(6.2) \quad P_p = I_p E_p = 50I_s$$

For example, at a secondary current of 0.5 amperes the primary electron heat load is 25 watts.

The heat load developed by the secondary electron current flowing through the diamond can be calculated very simply by

$$(6.3) \quad P_s = \int_{t_i}^{t_f} I_s \frac{E(t)}{\epsilon_r} V_d(t) dt$$

where $E(t)$ is the gun electric field at time t , $\epsilon_r=5.7$ is the dielectric constant of diamond and V_d is the drift velocity of the electrons, which acquires a time dependence through its dependence on the field strength. If we take a peak electric field in the gun (on the cathode) as 30 MV/m, a secondary phase of emission from the diamond as 30 degrees, a 10 microns thick diamond, the drift velocity as described in Section 5 and a secondary current of 0.5 amperes, the secondary electron heat load (calculated by integrating over the time dependence of the field) is 17 watts.

The temperature rise can be calculated given some dependence of the thermal conductivity on temperature [10]. We will approximate the thermal conductivity coefficient k (in units of W/m²K) in the temperature range of 100°K to 300°K as

$$(6.4) \quad k(T) \sim 14000 - 40T$$

This is a very crude approximation, meant just for the purpose of a rough estimate of the temperature increase in the diamond. Assuming that the edge of the diamond is at $T_e=100^\circ\text{K}$, and that the temperature rise is not bigger than 100°K , then we can integrate the temperature change across the diamond and get approximately

$$(6.5) \quad 14000(1 - 60T_e)\Delta T \sim \frac{P}{4\pi t}$$

or

$$(6.6) \quad \Delta T = \frac{P}{3.2 \times 10^4 \pi t} \sim 42$$

where P is the total power deposited, which for our example is 42 watts, and $t=10^{-5}$ meter is the thickness of the diamond. The result justifies the approximation made above. It shows that the excellent thermal conductivity of the diamond results a negligible temperature rise in the diamond window.

Increasing the thickness of the diamond improves the cooling and does not change P_p . The cooling and P_s are proportional to the diamond thickness. Thus, as long as P_p does not become negligible, the temperature rise at the center of the window will decrease with increasing thickness, tending to about 11°K .

The conductivity used above may be a bit on the optimistic side for a typical diamond sample. Indeed some samples are measured at room temperature to have a thermal conductivity half of the value used above. To estimate the worst possible case, we take the thermal conductivity value for the whole diamond as $1000 \text{ W/m}^\circ\text{K}$. This will result a temperature rise (center to edge) of 290 degrees, which is still quite comfortable.

References:

- [1] M. N. Yoder in *Applications of Diamond Films and related materials*, edited by Y. Tzeng et al., (Elsevier, NY 1991) , page 289
- [2] L. Krainsky, V. M. Asnin, J. A. Dayton, Appl. Surface Sc. 111, 265 (1997)
- [3] A. Hoffman et al., J. Appl. Phys. 91, 4726 (2002)
- [4] A. Shih et al. J. Appl. Phys. 82, 1860 (1997)
- [5] L. L. Krainsky et al. Phys. Rev. B 53, R7650 (1996)
- [6] E. M. Conwell, *High Field Transport in Semiconductors* (Academic Press, NY, 1967)
- [7] J. E. Yater, A. Shih, R. Abrams, Phys. Rev. B 56, R4410 (1997)
- [8] E. Worner et al. Diamond and Related Materials, 12, 744 (2003)
- [9] M. P. Seah and W. A. Dench, *Surf. Interface Anal.* 1, pg10 (1979)
- [10] D.G. Onn et al. Phys. Rev. Lett. 68 No. 18, 2806 (1992)